

# Higher Order Hierarchical Legendre Basis Functions for Electromagnetic Modeling

Erik Jørgensen, *Member, IEEE*, John L. Volakis, *Fellow, IEEE*, Peter Meincke, *Member, IEEE*, and Olav Breinbjerg, *Member, IEEE*

**Abstract**—This paper presents a new hierarchical basis of arbitrary order for integral equations solved with the method of moments (MoM). The basis is derived from orthogonal Legendre polynomials which are modified to impose continuity of vector quantities between neighboring elements while maintaining most of their desirable features. Expressions are presented for wire, surface, and volume elements but emphasis is given to the surface elements. In this case, the new hierarchical basis leads to a near-orthogonal expansion of the unknown surface current and implicitly an orthogonal expansion of the surface charge. In addition, all higher order terms in the expansion have two vanishing moments. In contrast to existing formulations, these properties allow the use of very high-order basis functions without introducing ill-conditioning of the resulting MoM matrix. Numerical results confirm that the condition number of the MoM matrix obtained with this new basis is much lower than existing higher order interpolatory and hierarchical basis functions. As a consequence of the excellent condition numbers, we demonstrate that even very high-order MoM systems, e.g., tenth order, can be solved efficiently with an iterative solver in relatively few iterations.

**Index Terms**—Basis functions, hierarchical systems, high-order methods, integral equations, method of moments (MoM), orthogonal functions, polynomial approximation.

## I. INTRODUCTION

ELECTROMAGNETIC integral equations are often discretized with the method of moments (MoM) [1] which is one of the most widespread and generally accepted techniques for electromagnetic problems. The MoM requires less unknowns than techniques based on differential equations but at the same time necessitates the solution of a matrix system with a dense and often ill-conditioned matrix [2]. With  $N$  being the number of basis functions, the solution time of the matrix system is proportional to  $N^3$  if a direct solver is applied,  $N^2$  with iterative solvers, or  $N \log(N)$  with accelerated iterative methods [3]. Thus, any efficient MoM technique must apply an iterative method. This requires a set of basis functions that does not lead to an ill-conditioned matrix. An increased accuracy of the solution and/or a reduced number of unknowns can be obtained by employing higher order basis functions.

Manuscript received February 20, 2003; revised January 27, 2004.

E. Jørgensen was with the Technical University of Denmark, DK-2800 Lyngby, Denmark. He is now with TICRA, DK-1201 Copenhagen K, Denmark (e-mail: ej@ticra.com).

J. L. Volakis is with the ElectroScience Laboratory, Electrical Engineering Department, The Ohio State University, Columbus, OH 43212 USA (e-mail: volakis.1@osu.edu).

P. Meincke and O. Breinbjerg are with the Technical University of Denmark, Ørsted-DTU, Electromagnetic Systems, DK-2800 Lyngby, Denmark (e-mail: pme@oersted.dtu.dk; ob@oersted.dtu.dk).

Digital Object Identifier 10.1109/TAP.2004.835279

Divergence-conforming basis functions that impose normal continuity of a vector quantity between neighboring elements, such as the electric surface current density, are usually applied in MoM [4]–[11] whereas curl-conforming functions that impose tangential continuity are applied in the finite element method (FEM) [8], [12]–[15]. The higher order functions can be categorized as interpolatory or hierarchical. The interpolatory ones, e.g., [8], interpolate the value of a field quantity at a number of interpolation points such that only one function is nonzero at the interpolation points. This allows a direct physical interpretation of the unknown coefficients but also limits the applicability of the basis since the expansion order must be kept constant throughout the mesh, thus requiring a mesh with equally sized elements. Hierarchical functions, e.g., [5], allow for much greater flexibility. The basis of order  $M$  is a subset of the basis of order  $M + 1$  which enables different expansion orders on different elements in the same mesh. Thus, a hierarchical basis includes the low-order basis, e.g., Rao–Wilton–Glisson (RWG) [16] or rooftop, as the lowest order member of the basis. As a consequence, hierarchical bases combine the advantages of both low-order and higher order bases into a single flexible basis.

The divergence-conforming higher order basis functions [5], [8] suffer from the undesirable side-effect of an ill-conditioned system matrix. Ill-conditioning is often worse with hierarchical functions than with interpolatory ones which has motivated many authors to use the latter, thus sacrificing the flexibility of the hierarchical functions. However, the results presented in [17] suggest that ill-conditioning can be avoided by making the basis functions near-orthogonal. Complete orthogonality is apparently not possible when the hierarchical expansion is required to satisfy continuity of the normal component across element boundaries. Orthogonality was not addressed previously in the context of higher order bases for MoM [4]–[10], except for [11] that investigated various orthogonal polynomials. However, the modification that was applied to enforce continuity essentially destroyed the orthogonality of the expansion. In the FEM context, Webb [15] used partial Gram–Schmidt orthogonalization to derive a set of hierarchical functions. However, this approach will lead to a worse result than the one presented here as will be explained in Section II-B.

In this paper, we develop a set of higher order hierarchical basis functions that provides a lower condition number than that of existing interpolatory functions and hierarchical functions. In fact, the condition number remains almost constant for increasing polynomial order. This is achieved in three steps

that differ from previous works. First, orthogonal Legendre polynomials are applied and second, a new procedure to modify the polynomials is used [18]. This allows for enforcing the continuity without destroying the orthogonality. Third, a further improvement of the matrix condition number is obtained by defining appropriate scaling factors that multiply each basis function. These scaling factors have a significant impact on the condition number but were not considered in previous works on hierarchical basis functions in the MoM context [4]–[6], [9]–[11]. Further, the modified Legendre polynomials implicitly yield an orthogonal expansion of the charge. To the knowledge of the authors, this feature has not been introduced in any of the works on higher order basis functions [4]–[15]. As a result of the low condition number, MoM matrix systems with even tenth-order Legendre basis functions can be solved iteratively.

Higher order basis functions enable large elements which calls for higher order curvilinear geometry modeling. Several authors have treated higher order curvilinear surface modeling for both low-order [19]–[21] and higher order [8], [22] basis functions. The functions presented here can be applied on curvilinear patches of arbitrary order and numerical results will be presented for curved second-order nine-node quadrilaterals. Quadrilaterals are preferred over triangular patches since they generally result in the lowest number of unknown. However, it simplifies the meshing task if a few triangles are allowed in a quadrilateral mesh. This is accomplished by simply treating triangles as degenerate quadrilaterals with two vertices collapsed into one.

This paper is organized as follows. Section II-A describes orthogonality properties of MoM basis functions. Section II-B presents the derivation of the basis functions for quadrilaterals with the properties of these functions discussed in Section II-C. Section II-D deals with the efficient calculation of the MoM matrix elements, whereas Sections II-E and II-F are devoted to generalizations for other elements shapes, i.e., triangular patches, wires, and hexahedral volumes. Section III presents validations and numerical results and Section IV includes some concluding remarks.

## II. NEW HIERARCHICAL LEGENDRE BASIS FUNCTIONS

### A. Orthogonality of Basis Functions in the MoM

The MoM is a general method for solving equations of the type  $L^c \mathbf{f}^c = \mathbf{g}^c$ , where  $L^c$  is an integro-differential operator,  $\mathbf{g}^c$  is a known vector function, and  $\mathbf{f}^c$  is an unknown vector function. The superscript  $c$  is used here to indicate that these functions are continuous. Discretizing the equation via the MoM yields the matrix equation  $[\bar{\mathbf{L}}]\{\mathbf{f}\} = \{\mathbf{g}\}$  in which

$$L_{ij} = \langle \mathbf{T}_i, L^c \mathbf{B}_j \rangle \quad (1a)$$

$$g_i = \langle \mathbf{T}_i, \mathbf{g}^c \rangle \quad (1b)$$

where  $\mathbf{T}_i$  and  $\mathbf{B}_j$  refer to the  $i$ th testing and  $j$ th basis functions, respectively. The inner product  $\langle \cdot, \cdot \rangle$  is defined as

$$\langle \mathbf{x}, \mathbf{y} \rangle = \int_S \mathbf{x}^* \cdot \mathbf{y} dS, \quad (2)$$

where the  $*$  denotes complex conjugation. For later use, we also define the matrix  $[\bar{\mathbf{S}}]$  as the inner products of the testing and basis functions

$$S_{ij} = \langle \mathbf{T}_i, \mathbf{B}_j \rangle. \quad (3)$$

The matrix  $[\bar{\mathbf{L}}]$  must be well-conditioned to successfully solve for  $\{\mathbf{f}\}$  using iterative methods. As is well-known, the matrix condition numbers depends on the eigenvalues of  $[\bar{\mathbf{L}}]$  which in turn are associated with the choice of testing and basis functions. However, it was shown in [17] that the eigenvalues of  $[\bar{\mathbf{S}}]^{-1}[\bar{\mathbf{L}}]$  approximate a subset of the continuous operator  $L^c$ , provided that the basis functions can accurately represent the eigenfunctions of the continuous operator. Thus, the eigenvalues of  $[\bar{\mathbf{S}}]^{-1}[\bar{\mathbf{L}}]$  are independent of the choice of testing and basis functions. Based on this, it was argued in [17] that the moment matrix  $[\bar{\mathbf{L}}]$  is well-conditioned if we choose basis and testing functions that yields a well-conditioned  $[\bar{\mathbf{S}}]$ . This is accomplished with first-order subsectional basis and testing functions, such as RWGs or rooftops, since  $[\bar{\mathbf{S}}]$  will be close to a diagonal matrix due to the disjoint supports of the basis and testing functions. However, for higher order basis functions the number of functions with common or overlapping supports can be very large, e.g., larger than 100, implying a larger bandwidth for the matrix  $[\bar{\mathbf{S}}]$ . This larger bandwidth is likely to produce a poorly conditioned  $[\bar{\mathbf{S}}]$ , and thus a poorly conditioned MoM matrix  $[\bar{\mathbf{L}}]$ . This argumentation explains why higher order basis functions may produce ill-conditioned MoM matrices. Nevertheless, there are ways to avoid ill-conditioned  $[\bar{\mathbf{S}}]$  matrices. Specifically, if the functions with common or overlapping supports satisfy the orthogonality relation

$$\langle \mathbf{T}_i, \mathbf{B}_j \rangle = 0 \quad \text{for } i \neq j \quad (4)$$

the  $[\bar{\mathbf{S}}]$  matrix will be well-conditioned due to its narrow bandwidth. To take advantage of the benefits brought by the higher order basis functions, it is therefore important to develop basis functions that are orthogonal in the sense defined by (4). In the following section we derive a near-orthogonal set of basis functions, so that  $[\bar{\mathbf{S}}]$  has few nonzero elements outside the diagonal.

### B. Construction of the Basis for Quadrilaterals

We consider a curved quadrilateral patch of arbitrary order with an associated parametric curvilinear coordinate system defined by  $-1 \leq u, v \leq 1$  (see Appendix I). The surface current on each patch is expanded as

$$\mathbf{J}_s = J_s^u \mathbf{a}_u + J_s^v \mathbf{a}_v \quad (5)$$

where  $\mathbf{a}_u$  and  $\mathbf{a}_v$  are the co-variant unitary vectors  $\mathbf{a}_u = \partial \mathbf{r} / \partial u$  and  $\mathbf{a}_v = \partial \mathbf{r} / \partial v$ . Without loss of generality we consider only  $u$ -directed currents with the understanding that  $v$ -directed currents can be obtained by interchanging  $u$  and  $v$ . Let us introduce the higher order expansion

$$J_s^u(u, v) = \frac{1}{\mathcal{J}_s(u, v)} \sum_{m=0}^{M^u} \sum_{n=0}^{N^v} a_{mn}^u P_m(u) P_n(v) \quad (6)$$

where  $\mathcal{J}_s(u, v) = |\mathbf{a}_u \times \mathbf{a}_v|$  is the surface Jacobian,  $a_{mn}^u$  are unknown coefficients, and  $P_m(u)$  and  $P_n(v)$  are expansion poly-

nomials. As will be shown later, the vector  $\mathbf{a}_u$  in (5) and the factor  $\mathcal{J}_s(u, v)$  in (6) are required by the curvilinear geometry modeling when normal continuity between elements is desired. However, they make it difficult to derive an orthogonal basis set for all possible patch shapes. Therefore, the following discussion about orthogonality is strictly related to the expansion polynomials  $P_m(u)$  and  $P_n(v)$ . Thus, the orthogonality of the basis functions is only maintained when  $\mathbf{a}_u/\mathcal{J}_s(u, v)$  has no  $u$  and  $v$  dependence, i.e., on rectangular or rhomboid-shaped patches. Nevertheless, the numerical results in Section III confirm that favorable condition numbers can also be obtained for more general patch shapes.

The choice of polynomials in (6) is important for the resulting matrix condition number. In [5], the power expansion  $P_m(u) = u^m$  was chosen. In this work we choose  $P_m(u)$  and  $P_n(v)$  to be the Legendre polynomials

$$P_m(u) = \frac{1}{2^m m!} \frac{d^m}{du^m} (u^2 - 1)^m \quad (7)$$

that satisfy the orthogonality relation

$$\int_{-1}^1 P_i(u) P_j(u) du = \frac{2}{2i + 1} \delta_{ij} \quad (8)$$

where  $\delta_{ij}$  is the Kronecker delta function.

The expansion in (6) is not appropriate if normal continuity of the current flowing across patch boundaries is to be enforced. Instead, the polynomials along the direction of current flow, i.e., the  $u$ -direction, must be modified such that only a single low-order polynomial is nonzero at the edge  $u = -1$ , a single low-order polynomial is nonzero at the edge  $u = 1$ , and the higher order polynomials are zero at both edges. This modification can be done in several different ways. To illustrate the properties of the modified polynomials discussed below we define a matrix  $[\tilde{\mathbf{S}}^{1D}]$  with the elements

$$S_{ij}^{1D} = \int_{-1}^1 P_i^{\text{mod}}(u) P_j^{\text{mod}}(u) du \quad (9)$$

where  $P_i^{\text{mod}}(u)$  are the modified polynomials to be defined. This matrix should preferably be a diagonal matrix, indicating that the modified polynomials are orthogonal. However, complete orthogonality is not possible if the lowest order expansion ( $M^u = 1$ ) is required to be the rooftop functions  $1 \pm u$ . One possible modification was applied to a power expansion in [5] and later used with several different types of polynomials in [11]. Applying the same modification to the Legendre polynomials yields the modified polynomials

$$P_m^{\text{mod}}(u) = \begin{cases} 1 - u, & m = 0 \\ 1 + u, & m = 1 \\ P_m(u) - 1, & m = 2, 4, 6, \dots \\ P_m(u) - u, & m = 3, 5, 7, \dots \end{cases} \quad (10)$$

Unfortunately, the modified polynomials  $P_m^{\text{mod}}(u)$  obtained from this procedure are far from orthogonal, due to the subtracted terms for  $m \geq 2$  in (10). In fact, all higher order functions have nonzero inner products with the two lowest order functions, and all even (odd) higher order functions have

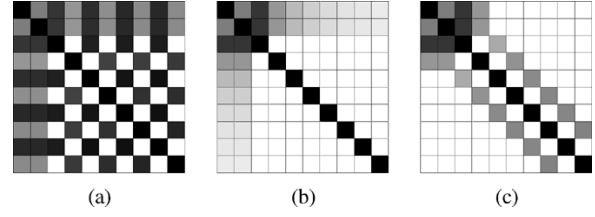


Fig. 1. Normalized inner product matrices  $[\tilde{\mathbf{S}}^{1D}]$  for the modified polynomials (linear scale), (a) the modified polynomials  $P_m^{\text{mod}}(u)$  in (10), (b) the modified polynomials  $P_m^{\text{mod}}(u)$  in (10) after Gram–Schmidt orthogonalization, and (c) the modified polynomials  $\tilde{P}_m(u)$  in (11).

nonzero inner products with all other even (odd) higher order functions. This is illustrated in Fig. 1(a) that shows the matrix  $[\tilde{\mathbf{S}}^{1D}]$  for the polynomials  $P_m^{\text{mod}}(u)$  for  $0 \leq m \leq 10$ . As seen, the coupling between odd and even polynomials results in a large number of nonzero elements, indicating that the orthogonality of the Legendre polynomials have been destroyed by the modification.

The lack of orthogonality can be avoided by using partial Gram–Schmidt orthogonalization, as in [15], to orthogonalize all higher order functions. Nevertheless, this approach cannot be used to orthogonalize the higher order functions with respect to the two lowest order functions  $1 \pm u$ , since this would destroy the necessary property  $P_m^{\text{mod}}(\pm 1) = 0, m \geq 2$ . This is illustrated in Fig. 1(b) that shows the matrix  $[\tilde{\mathbf{S}}^{1D}]$  obtained by applying Gram–Schmidt orthogonalization to the modified polynomials in (10). The nonzero elements in the first two rows and columns indicate the nonzero inner products of the higher order polynomials with the two lowest-order polynomials,  $1 \pm u$ .

Instead of the modifications described above, we propose the alternative modified higher order polynomials

$$\tilde{P}_m(u) = \begin{cases} 1 - u, & m = 0 \\ 1 + u, & m = 1 \\ P_m(u) - P_{m-2}(u), & m \geq 2 \end{cases} \quad (11)$$

that have the desired property  $\tilde{P}_m(\pm 1) = 0, m \geq 2$ . The idea of subtracting two Legendre polynomials was also applied in [23] to formulate scalar entire-domain basis functions for differential equations. However, the vectorial subsectional basis functions derived here differ significantly from those of [23]. For  $m \geq 4$  the modified polynomials in (11) are orthogonal to the two lowest order functions,  $1 \pm u$ . However, all higher order polynomials have nonzero inner products with the polynomials two orders lower and two orders higher. This is illustrated in Fig. 1(c) that shows the matrix  $[\tilde{\mathbf{S}}^{1D}]$  for the modified polynomials in (11). By comparing the three matrices in Fig. 1, we observe that this latter modification provides the lowest number of nonzero terms and a diagonally strong  $[\tilde{\mathbf{S}}^{1D}]$ . Thus, the orthogonality of the Legendre polynomials is best preserved by applying the modification in (11). We also remark that the modified polynomials obtained by the Gram–Schmidt orthogonalization do not possess the desirable features derived from (18)–(23) in Sections II-C and II-D.

The next step is to determine appropriate scaling factors for the basis functions that minimize the condition number. Numerical experiments showed that a good choice is to scale such that the Euclidean norm of each basis function is unity on a square

patch of unit side length. The experiments verified that other options, e.g., scaling each function to a maximum value of 1, did not perform equally well. By defining the scaling factors

$$\tilde{C}_m = \begin{cases} \frac{\sqrt{3}}{4}, & m = 0, 1 \\ \frac{1}{2} \sqrt{\frac{(2m-3)(2m+1)}{2m-1}}, & m \geq 2 \end{cases} \quad (12a)$$

$$C_n = \sqrt{n + \frac{1}{2}} \quad (12b)$$

and inserting the modified polynomials  $\tilde{P}_m(u)$  in the initial expansion (6), the obtained final expansion is

$$J_s^u(u, v) = \frac{1}{\mathcal{J}_s(u, v)} \sum_{m=0}^{M^u} \sum_{n=0}^{N^v} b_{mn}^u \tilde{C}_m \tilde{P}_m(u) C_n P_n(v) \quad (13)$$

where  $b_{mn}^u$  are the new unknown coefficients. An alternative representation that separates the functions which take part in maintaining the normal continuity and the functions which are zero at  $u = \pm 1$  is

$$J_s^u(u, v) = \frac{1}{\mathcal{J}_s(u, v)} \sum_{n=0}^{N^v} \left[ b_{0n}^u (1-u) + b_{1n}^u (1+u) \right] \tilde{C}_0 C_n P_n(v) + \frac{1}{\mathcal{J}_s(u, v)} \sum_{m=2}^{M^u} \sum_{n=0}^{N^v} b_{mn}^u \tilde{C}_m \tilde{P}_m(u) C_n P_n(v). \quad (14)$$

In the next section, we examine the properties of the above expansion.

### C. Properties of the Expansion

In (14), the polynomials with a  $u$ -dependence were modified to incorporate normal continuity across patch edges. To be specific, the functions in the first line of (14) have a linear variation in the  $u$ -direction and are nonzero at  $u = 1$  or  $u = -1$ . These functions serve to ensure the normal continuity across the  $v$ -directed edges and must be matched with similar functions on the neighboring patch. For this reason, these functions are sometimes referred to as edge functions or doublets. The normal component of the basis functions will be continuous, provided that  $\mathbf{a}_u/\mathcal{J}_s$  is the same on both sides of any common edge of two neighboring patches. Using the results (36b) and (38) from Appendix II, the normal component of  $\mathbf{a}_u/\mathcal{J}_s$  across a  $v$ -directed edge is

$$\frac{\mathbf{a}_u}{\mathcal{J}_s} \cdot \frac{\mathbf{a}^u}{|\mathbf{a}^u|} = \frac{1}{\mathcal{J}_s |\mathbf{a}^u|} = \frac{1}{|\mathbf{a}_v|} \quad (15)$$

where  $\mathbf{a}^u$  is the contravariant unitary vector. The quantity  $|\mathbf{a}_v|$  remains the same on both sides of the edge since the vectors  $\mathbf{a}_v$  on two neighboring patches are tangential to the same edge. Thus, normal continuity is maintained when the surface Jacobian  $\mathcal{J}_s$  is included in the expansion.

The functions in the second line of (14) are zero at  $u = \pm 1$  and do not contribute to the normal continuity of the current. They are defined on a single patch and have an  $m$ th order polynomial variation in the  $u$ -direction, where  $m \geq 2$ . These functions are often referred to as patch functions or singletons.

The  $u$ -directed basis functions in (13) allow an independent selection of the expansion orders along the direction of current

flow ( $M^u$ ) and along the transverse direction ( $N^v$ ). Similarly, the  $v$ -directed basis functions not shown in (13) are characterized by the expansion orders along the direction of current flow ( $M^v$ ) and along the transverse direction ( $N^u$ ). A set of basis functions that is compatible with the Nedelec constraint [12] is obtained by choosing  $M^u = M^v = N^v + 1 = N^u + 1$ . Such functions are said to be of mixed-order since the order of the expansion along the direction of current flow is one order higher than along the transverse direction. The Nedelec constraint ensures a consistent charge expansion that is polynomial complete to order  $N^v = N^u$ . However, the Nedelec constraint is only a reasonable choice for near-square patches and turns out to be too restrictive for patches of more general shape. For such patches, the parameters  $M^u$  and  $M^v$  must be selected independently depending on the electrical size of the patch along the particular direction. Nevertheless, a consistent charge expansion is only obtained by maintaining the requirements  $M^u = N^u + 1$  and  $M^v = N^v + 1$ . The charge expansion is then polynomial complete to orders  $N^u$  and  $N^v$  along the  $u$ - and  $v$ -directions, respectively. These requirements can be seen as a generalized Nedelec constraint and our experience has shown that it works well in praxis. Particularly, by introducing these requirements in (13) and also including the  $v$ -directed currents we obtain

$$\mathbf{J}_s = \frac{1}{\mathcal{J}_s(u, v)} \left( \mathbf{a}_u \sum_{m=0}^{M^u} \sum_{n=0}^{M^v-1} b_{mn}^u \tilde{C}_m \tilde{P}_m(u) C_n P_n(v) + \mathbf{a}_v \sum_{m=0}^{M^v} \sum_{n=0}^{M^u-1} b_{mn}^v \tilde{C}_m \tilde{P}_m(v) C_n P_n(u) \right) \quad (16)$$

which should be used in practical implementations. The above expression contains all basis functions defined on a single patch and allows only two parameters to be selected,  $M^u$  and  $M^v$ . Note that the lowest order of approximation ( $M^u = M^v = 1$ ) yields the well-known rooftop functions.

It is also instructive to examine the orthogonality of the charge expansion which also appears in the MoM matrix elements. The charge associated with the  $u$ -directed currents can be obtained from the continuity equation as

$$\rho_s^u = \frac{1}{\mathcal{J}_s} \frac{j}{\omega} \frac{d}{du} (\mathcal{J}_s J_s^u) \quad (17)$$

and we note that for Legendre polynomials we have the identity

$$\frac{d}{du} (P_m(u) - P_{m-2}(u)) = \frac{d}{du} \tilde{P}_m(u) = (2m-1) P_{m-1}(u), \quad m \geq 2. \quad (18)$$

Substituting this into (17) yields

$$\begin{aligned} \rho_s^u(u, v) &= \frac{j}{\omega} \frac{1}{\mathcal{J}_s(u, v)} \sum_{n=0}^{N^v} \left[ -b_{0n}^u + b_{1n}^u \right] \tilde{C}_0 C_n P_n(v) \\ &\quad + \frac{j}{\omega} \frac{1}{\mathcal{J}_s(u, v)} \sum_{m=2}^{M^u} \sum_{n=0}^{N^v} b_{mn}^u (2m-1) \tilde{C}_m P_{m-1}(u) C_n P_n(v). \end{aligned} \quad (19)$$

The functions in the second line of this equation are all mutually orthogonal and orthogonal to the functions in the first line of the equation. Consequently, the current expansion in (14) implicitly yields a higher order orthogonal expansion of the charge. Note that this is only accomplished by using Legendre polynomials and modifying the polynomials as in (11). The significance of the orthogonal charge can be seen when the MoM matrix elements associated with the mixed-potential electric field integral equation (EFIE) with Galerkin testing is evaluated. With  $\mathbf{J}_s^i$  being the  $i$ th testing function and  $\mathbf{J}_s^j$  the  $j$ th expansion function, the matrix elements have the form

$$Z_{ij} = \langle \mathbf{J}_s^i, L_J(\mathbf{J}_s^j) \rangle - \frac{j}{\omega} \langle \nabla_s \cdot \mathbf{J}_s^i, L_\rho(\nabla_s \cdot \mathbf{J}_s^j) \rangle \quad (20)$$

where  $L_J(\cdot)$  is the electric field integral operator associated with the vector potential and  $L_\rho(\cdot)$  is the electric field integral operator associated with the scalar potential. The last inner product appearing in (20) is essentially the inner product of the charge associated with the testing function and the operator working on the charge associated with the expansion function. In analogy with the argumentation of Section II-A, this suggests that using an orthogonal expansion of the charge will contribute to a favorable condition number of the MoM matrix.

For Legendre polynomials we have the relations

$$\int_{-1}^1 P_n(v) dv = 0, \quad n > 0 \quad (21a)$$

$$\int_{-1}^1 v P_n(v) dv = 0, \quad n > 1 \quad (21b)$$

and for the modified polynomials these imply

$$\int_{-1}^1 \tilde{P}_m(u) du = 0, \quad m > 2 \quad (22a)$$

$$\int_{-1}^1 u \tilde{P}_m(u) du = 0, \quad m > 3. \quad (22b)$$

This property of vanishing moments can be used to estimate the far-zone field radiated by a higher order basis function. Using a first-order Taylor expansion of the slowly varying far-zone Green's function shows that all functions with  $m > 3$  or  $n > 1$  radiate zero far-zone field. In other words, the Legendre basis functions are carefully shaped to concentrate the far-zone interactions in the low-order functions, whereas the higher order terms mostly act as local corrections. This is a fundamental aspect of the proposed basis functions and ensures the strong diagonal property of the MoM matrix.

#### D. Matrix Element Evaluation

Explicit expressions for the MoM matrix elements will not be given here since they depend on the type of integral equation being solved. It is worth noting however, that for the particular case of a mixed-potential electric field surface integral equation with Galerkin testing, we do not need to evaluate  $\mathcal{J}_s(u, v)$  in (14) since this term is canceled by the differential surface element  $dS = \mathcal{J}_s(u, v) du dv$ . Specifically, the  $\mathcal{J}_s(u, v)$  of the testing function is canceled by the  $dS$  appearing in the inner product in (20), whereas the  $\mathcal{J}_s(u, v)$  of the basis function is canceled by the  $dS$  of the integral operator.

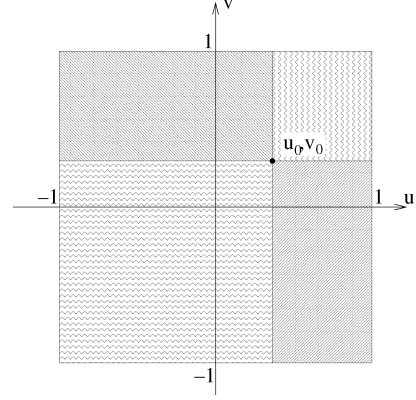


Fig. 2. Illustration of the annihilation procedure. The quadrilateral patch with a singularity at  $(u_0, v_0)$  is mapped into four smaller patches, each with a singularity at the origin.

When implementing (14), the Legendre polynomials are efficiently calculated by the recurrence formula

$$P_m(u) = \frac{1}{m} [(2m-1)uP_{m-1}(u) - (m-1)P_{m-2}(u)]. \quad (23)$$

Equations (23) and (18) imply, that by computing the basis functions of order  $M^u$ , as a byproduct we have also computed the basis functions of all lower orders, as well as their corresponding charges.

Numerical evaluation of the self-term matrix elements is often based on extraction of the singular part of the integrand. However, in the case of higher order functions and curved patches this approach is extremely tedious and leads to complicated expressions for the singular part of the integrand. A better choice is the purely numerical annihilation procedure that is based on the Duffy transform [24] and was applied to hexahedrals in [25]. This procedure can be adapted to surface quadrilaterals as described below.

Consider the generic integral

$$I = \int_{-1}^1 \int_{-1}^1 f(u, v) G(u, v, u_0, v_0) du dv \quad (24)$$

where  $f$  is a well-behaved arbitrary function and  $G(u, v, u_0, v_0)$  is some other function with a first order singularity at  $(u, v) = (u_0, v_0)$ . The original integration domain is now mapped into four new domains, each with a vertex at  $(u_0, v_0)$ , as illustrated in Fig. 2. By using four different linear mappings, (24) can be cast into the form

$$I = \sum_{i=1}^4 \int_0^1 \int_0^1 f_i(\zeta, \eta) G_i(\zeta, \eta) J_i d\zeta d\eta \quad (25)$$

where  $J_i$  is the Jacobian of the linear mapping. By applying the transformation  $\zeta = \alpha^2$  and  $\eta = \beta^2$  we obtain

$$I = \sum_{i=1}^4 \int_0^1 \int_0^1 f_i(\alpha^2, \beta^2) G_i(\alpha^2, \beta^2) J_i 4\alpha\beta d\alpha d\beta \quad (26)$$

where  $G$  after the transformation has a second order singularity at  $(\alpha, \beta) = (0, 0)$ . However, this singularity is canceled by

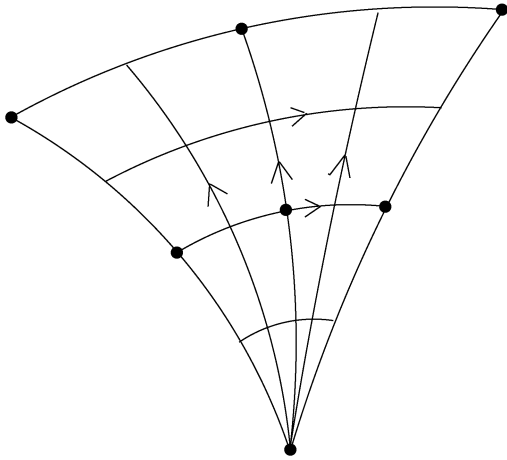


Fig. 3. Coordinate lines on a seven-node second-order triangle represented as a degenerate nine-node second-order quadrilateral.

the term  $\alpha\beta$ . Thus, the four integrands in (26) are all well-behaved and can be integrated using a standard Gaussian quadrature method. The annihilation procedure is an excellent tool for writing very general codes since the functions  $f$  and  $G$  are arbitrary. Thus, the same code can be used without modifications for a variety of basis functions and Green's functions. This is not possible with methods based on analytical singularity extraction.

#### E. Triangles in a Quadrilateral Mesh

The geometrical segmentation in terms of quadrilateral patches of arbitrary order (Appendix I) can represent most objects with sufficient accuracy. However, it simplifies meshing of complicated structures if the numerical method allows a few triangular patches in a quadrilateral mesh. Introducing special basis functions on triangles would complicate the practical implementation significantly. Instead, we propose here to simply maintain the standard quadrilateral basis function and treat triangles as degenerate quadrilaterals with two vertices collapsed into one. Naturally, an edge with zero length should not have a normal current component flowing across it, which can be enforced by treating the edge as an external edge. The  $u$  and  $v$  coordinate lines on such a degenerate quadrilateral are shown in Fig. 3. It is observed that the three edges are not treated symmetrically since one current component flows between two edges whereas the other current component flows from a vertex to an edge. Numerical experiments have verified that this does not introduce numerical instabilities, and that the accuracy is comparable to basis functions specifically defined on triangles.

#### F. Generalization to Wires and Volumes

The basis functions defined in the previous subsections were given for surface patches. However, it is straightforward to generalize them to wires and volumes. Specifically, the current on a wire can be expanded as

$$I(u) = \sum_{m=0}^M b_m \tilde{C}_m \tilde{P}_m(u). \quad (27)$$

For a curvilinear hexahedral volume with the parametric coordinates  $(u, v, w)$ , the electric flux density  $\mathbf{D}$  can be written in terms of its contravariant components as

$$\mathbf{D}(u, v, w) = D^u \mathbf{a}_u + D^v \mathbf{a}_v + D^w \mathbf{a}_w \quad (28)$$

where  $\mathbf{a}_w = \partial \mathbf{r} / \partial w$  is the covariant unitary vector in the  $w$ -direction. A divergence-conforming expansion of the  $D^u$  component is then

$$D^u(u, v, w) = \frac{1}{\mathcal{J}(u, v, w)} \cdot \sum_{m=0}^{M^u} \sum_{n=0}^{M^v-1} \sum_{q=0}^{M^w-1} b_{mnq}^u \tilde{C}_m \tilde{P}_m(u) C_n P_n(v) C_q P_q(w) \quad (29)$$

where  $\mathcal{J}$  is the Jacobian

$$\mathcal{J} = \mathbf{a}_u \cdot \mathbf{a}_v \times \mathbf{a}_w. \quad (30)$$

The components  $D^v$  and  $D^w$  can be expanded in a similar way by interchanging  $(u, v, w)$  in a cyclic fashion. The basis functions for wires and volumes have the same favorable orthogonality properties as the surface functions in (14). Thus, they are expected to provide similar improvements of the condition number when compared to other higher order expansions, e.g., [8], [26].

All the basis functions presented above are divergence-conforming and allows to impose normal continuity of a vector quantity across element boundaries. Similar curl-conforming basis functions for imposing tangential continuity can be obtained by using the contravariant unitary vectors [see Appendix II, (35)]. Such functions are suitable for the finite element method (FEM) or in volumetric integral equation solvers when the electric field is the unknown.

### III. NUMERICAL RESULTS

The advantages of higher order basis functions have already been mentioned in the literature [4]–[10]. Particularly, convergence results were reported for spheres in [27] and for flat plates in [28]. The presence of sharp edges has some impact on the accuracy but even in this case, higher order basis functions provide better convergence than low-order basis functions. This was shown in [29] that also presented an extension of the higher order Legendre basis functions that incorporates edge singularities. Typically, use of higher order basis functions allows the number of unknowns to be reduced by a factor of 4–5. However, due to the increased condition number of the MoM matrix an iterative solver may need more iterations for convergence and this has compromised the effectiveness of the higher order basis functions. Thus, we choose here to focus on the condition number of the MoM system when using higher order basis functions. To this end we apply a standard MoM solution with Galerkin testing to three simple perfectly conducting geometrical objects; these are two parallel plates, two parallel circular discs, and a pyramid. The condition number is higher when geometrical singularities such as corners and edges are present. Furthermore, the condition number is strongly affected by over-discretization. Thus, the geometrical objects are chosen to incorporate geometrical singularities with over-discretization to ob-

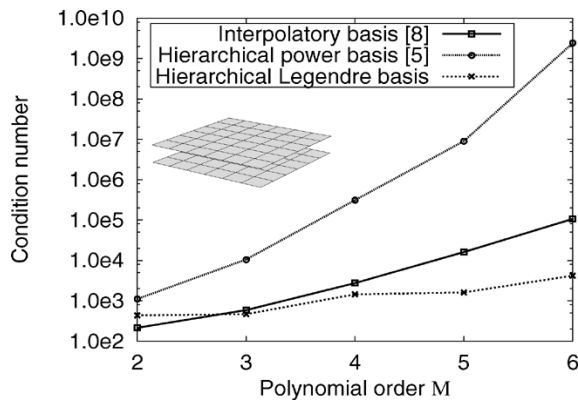


Fig. 4. EFIE condition numbers for the  $6\lambda \times 6\lambda$  parallel plates. The interpolatory basis of [8] is compared to the hierarchical basis of [5] and the hierarchical Legendre basis developed in this paper.

TABLE I  
SIZE OF SQUARE PATCHES AND THE NUMBER OF UNKNOWNNS FOR THE  $6\lambda \times 6\lambda$  PARALLEL PLATES

Pol. order $M$	2	3	4	5	6
Patch size ( $\lambda$ )	0.38	0.6	0.86	1.0	1.2
Unknowns	3968	3480	3024	3480	3480

tain a worst-case scenario. In each case, the condition number for increasing polynomial order is obtained. Further, to isolate the effect of increasing the polynomial order, we have tried to keep the number of unknowns constant, or slightly decreasing, by increasing the patch size along with the polynomial order. We compare our hierarchical Legendre basis functions with two existing types of higher order basis functions; the hierarchical functions of [5] based on a power expansion, and the interpolatory ones of [8] based on Lagrange polynomials. The scaling factors given in (12) and those suggested in [8] are essential for realizing a low condition number and these factors are included in the analysis (no scaling factors were suggested in [5]). The choice  $M^u = M^v = N^v + 1 = N^u + 1$  are used throughout this section which realizes a basis compatible with the Nedelec constraint. Furthermore, this choice ensures that the basis functions presented here and those of [5] and [8] all span the same polynomial space and involve the same number of unknowns for a given polynomial order. The surface current densities obtained with the three types of basis functions are therefore identical for a fixed polynomial order and only the condition numbers of the MoM matrices differ. In the following we do not distinguish between the  $u$ - and  $v$ -directions and simply refer to the polynomial order as  $M = M^u = M^v$ . Results are presented for both the EFIE and the combined field integral equation (CFIE).

First, we consider the two  $6\lambda \times 6\lambda$  parallel plates with  $1\lambda$  separation shown in the inset of Fig. 4. The three types of basis functions are applied in the EFIE and the 2-norm condition number is obtained for polynomial orders between  $M = 2$  and  $M = 6$ . The patch size and number of unknowns are the same with the three types of basis functions and listed in Table I. The condition numbers are graphed in Fig. 4 and the hierarchical Legendre basis functions presented here provide for an almost constant condition number as the polynomial order increases. However, at the same time, the condition numbers of [5] and [8] grow

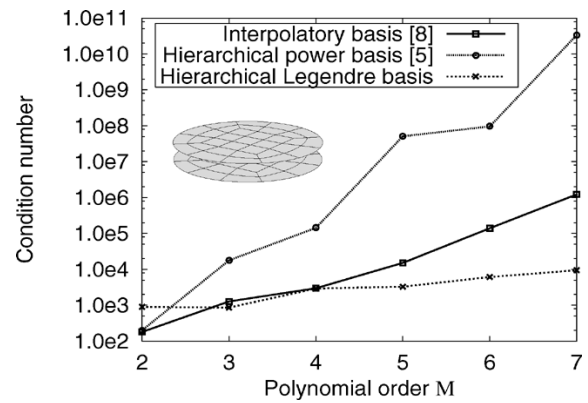


Fig. 5. Condition numbers for two parallel discs with diameter  $10\lambda$  and  $1\lambda$  separation. The interpolatory basis of [8] is compared to the hierarchical basis of [5] and the hierarchical Legendre basis developed in this paper.

TABLE II  
AVERAGE PATCH SIZE AND NUMBER OF UNKNOWNNS FOR THE PARALLEL DISCS

Pol. order $M$	2	3	4	5	6	7
Average patch size ( $\lambda$ )	0.5	0.83	1.08	1.35	2.10	2.10
Unknowns	10200	7992	8400	8400	4680	6384

much faster. Particularly, the condition number obtained with the hierarchical basis functions of [5] grows approximately one order of magnitude for each polynomial order.

The discussion on orthogonality in Section II-B was limited to rectangular or rhomboid shaped patches. To show that the favorable condition numbers are maintained for more general patch shapes, we apply the aforementioned three different basis functions to two parallel discs with a diameter of  $10\lambda$  and a  $1\lambda$  separation, as shown in the inset of Fig. 5. The patches are the nine-node quadrilaterals with curved edges with average patch size and number of unknowns for varying polynomial order as listed in Table II. The condition numbers obtained with the EFIE are shown in Fig. 5. Again, the hierarchical Legendre basis functions of this paper provide for an almost constant condition number whereas the bases of [5] and [8] result in rapidly growing condition numbers for increasing polynomial degree. In fact, by increasing the polynomial order from 2 to 7 the condition number obtained with the interpolatory basis displays an increase by approximately 4 orders of magnitude whereas the condition number obtained with our proposed basis does not even increase by a factor of 10.

The EFIE, being a first-kind integral equation, always suffers more from ill-conditioning than the CFIE. Thus, the CFIE is preferable for closed structures such as the pyramid in Fig. 6. A high condition number is expected for this object due to its sharp edges and the irregularly shaped patches. The condition number obtained with  $M = 4, 5,$  and  $6$  are listed in Table III for the basis of this paper and for the interpolatory basis [8]. Clearly, for the CFIE the growth in condition number with increasing polynomial order is much lower than that of the EFIE. Nevertheless, the observations given above for the EFIE still apply here.

The results given above show that hierarchical Legendre basis functions of very high orders can be applied without compromising the condition number of the MoM matrix. Thus, an efficient iterative equation solver can most likely be employed

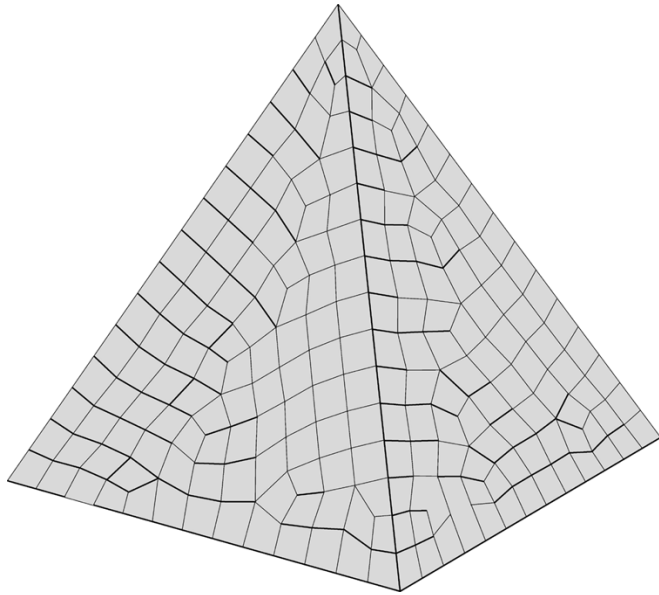


Fig. 6. Mesh of a pyramid with side length  $10\lambda$ .

TABLE III  
AVERAGE PATCH SIZE, NUMBER OF UNKNOWNNS, AND THE RESULTING  
CONDITION CFIE NUMBER FOR THE PYRAMID

Pol. order $M$		4	5	6
Average patch size ( $\lambda$ )		0.8	1.2	1.2
Unknowns		18656	11800	16992
Cond. number	This paper	425	724	1332
	[8]	1547	7680	79846

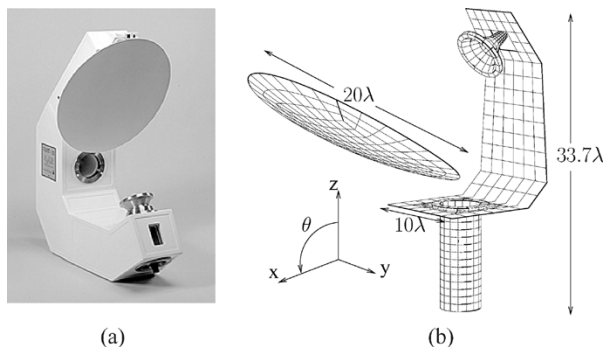


Fig. 7. Shaped offset reflector antenna (a), and (b), mesh of the reflector, feed horn, and that part of the mounting structure contributing to the field for  $\theta > 0$ . The mesh contains both four- and nine-node curvilinear quadrilaterals with sizes ranging from  $0.1\lambda$  to  $2.2\lambda$ . The total surface area is  $851\lambda^2$ .

with the same success as for the low-order basis. To demonstrate this for a more realistic problem we consider the configuration shown in Fig. 7. This is a shaped offset reflector antenna having a reflector diameter of  $20\lambda$ . This antenna is a validation standard used by the European Space Agency (ESA) for calibrating measurement facilities. The model includes a part of the antenna mounting structure and the feed horn. This configuration involves both large smooth regions and small geometrical details with subwavelength extent. Low-order basis functions, e.g., RWGs, would result in a large number of unknowns since they require small patches even in smooth regions. The mesh of the shaped reflector and the mounting structure is

shown in Fig. 7. Both four- and nine-node curvilinear quadrilaterals are used and the patch size is between  $0.1\lambda$  and  $2.2\lambda$ . Using our hierarchical Legendre basis functions the polynomial order is selected independently on each patch and is between  $M = 1$  and  $M = 10$  resulting in 21 264 unknowns in total. This corresponds to an average basis function density of 25 per square wavelength. The iterative algorithm employs an efficient near-neighbor preconditioner with overlapping domains which are necessary due to the very large patches [30]. Despite the application of tenth-order basis functions in the EFIE, the solution converged to a relative residual error of  $10^{-4}$  in only 79 GMRES [31] iterations. The radiation pattern of the antenna is strongly affected by the presence of the mounting structure in the region  $\theta > 0$  which can be seen in Fig. 8. The agreement with measured results is excellent when the mounting structure is included in the simulation. The measured data were obtained at the DTU-ESA Spherical Near-Field Antenna Test Facility at the Technical University of Denmark (DTU). To put the number of iterations into perspective, we can compare with an equivalent solution obtained with RWG basis functions. Solving the problem at hand requires more than 100 000 RWG functions. Consequently, the required memory and CPU time needed to perform a matrix-vector product are increased by approximately a factor of 20 in comparison to the higher order hierarchical Legendre basis functions. Thus, the RWG solution is not competitive in terms of memory and must converge within an unlikely 4 iterations to be competitive in terms of CPU time.

#### IV. CONCLUSION

A new set of higher order hierarchical Legendre basis functions was proposed for expanding electromagnetic fields or currents in differential or integral-equation based solution methods. Expressions of the divergence-conforming functions for moment method implementations were given for wires, surfaces, and volumes but the curl-conforming versions, e.g., for application in the FEM, can easily be obtained. The new basis is constructed by modifying the Legendre polynomials in a way that preserves almost perfect orthogonality while enforcing continuity of the normal current component across surface element edges. As a result of this procedure, the surface charge is implicitly expanded in orthogonal functions. In addition, the higher order functions can easily be computed for arbitrary orders and have two vanishing moments which implies a relatively low far-field contribution from these functions. Due to their hierarchical property, the proposed basis functions have all the advantages of both low-order and higher order basis functions. Numerical experiments have shown that the new basis functions provide for a much better condition number of the MoM matrix than available higher order hierarchical and higher order interpolatory basis functions. This enables efficient iterative solution of higher order MoM systems which are also much smaller than corresponding low-order systems. As a consequence, both memory requirements and computation time will be very low. The given numerical examples demonstrated the use of first- to tenth-order hierarchical functions on second-order curved surface patches where convergence were obtained in relatively few iterations.

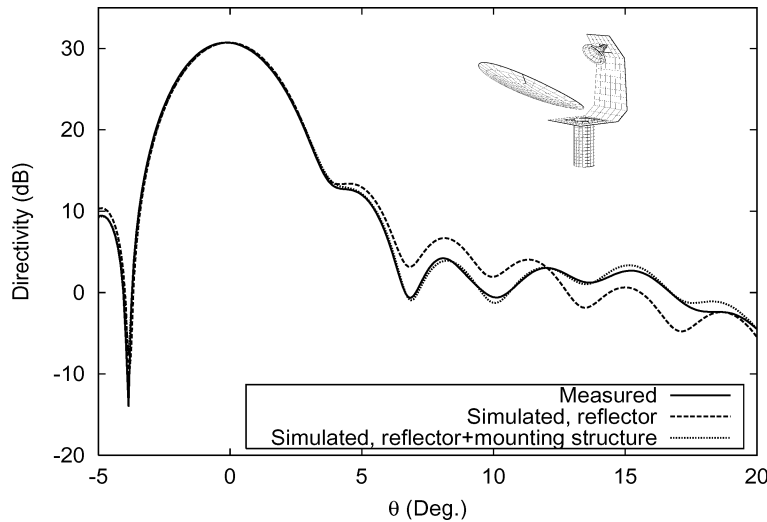


Fig. 8. Co-polar radiation pattern in the  $xz$ -plane for the shaped reflector antenna compared to the simulation results obtained with hierarchical Legendre basis functions. The simulations are done both with and without the mounting structure which has a significant effect on the radiation pattern for  $\theta > 0$ .

APPENDIX I

QUADRILATERAL PATCHES OF ARBITRARY ORDER

Consider a generalized quadrilateral patches with a curvilinear parametric  $(u, v)$  coordinate systems defined by  $-1 \leq u, v \leq 1$ . The generalized quadrilateral of order  $p$  given by  $(p + 1)^2$  interpolation nodes can be written as [32]

$$\mathbf{r}(u, v) = \sum_{i=0}^p \sum_{j=0}^p \mathbf{r}_{ij} \phi_i(p, u) \phi_j(p, v) \quad (31)$$

where  $\mathbf{r}_{ij}$  are the interpolation nodes and  $\phi_i(p, u)$  is the  $i$ th Lagrangian function of order  $p$

$$\phi_i(p, u) = \prod_{\substack{k=0 \\ k \neq i}}^p \frac{u - u_k}{u_i - u_k} = \prod_{\substack{k=0 \\ k \neq i}}^p \frac{\frac{p}{2}(u+1) - k}{i - k}. \quad (32)$$

Here  $u_k$  is the parametric coordinate of the interpolation node and the last equality holds when  $p + 1$  equidistant  $u_k$  are chosen, i.e.,  $u_k = -1 + 2k/p$ . The representation in (31) allows a subsection of the actual surface to be approximated by a quadrilateral patch of arbitrary order. For practical reasons, the most commonly used patches are bilinear quadrilaterals given by four nodes, or second-order quadrilaterals given by nine nodes. An alternative representation of (31) that facilitates mixing of patches with different orders in the same mesh is

$$\mathbf{r}(u, v) = \sum_{k=0}^p \sum_{l=0}^p \mathbf{r}_{kl} u^k v^l \quad (33)$$

where  $\mathbf{r}_{kl}$  are constant vectors given by a linear combination of the interpolation nodes  $\mathbf{r}_{ij}$ . The latter can be easily identified by inserting (32) in (31).

APPENDIX II

COVARIANT AND CONTRAVARIANT UNITARY VECTORS

We define the covariant unitary vectors as

$$\mathbf{a}_u = \frac{\partial \mathbf{r}}{\partial u}, \quad \mathbf{a}_v = \frac{\partial \mathbf{r}}{\partial v} \quad (34)$$

and the contravariant unitary vectors as

$$\mathbf{a}^u = \nabla u, \quad \mathbf{a}^v = \nabla v. \quad (35)$$

It is straightforward to show the relations

$$\mathbf{a}_u \cdot \mathbf{a}^u = 1, \quad \mathbf{a}_v \cdot \mathbf{a}^v = 1 \quad (36a)$$

$$\mathbf{a}_u \cdot \mathbf{a}^v = 0, \quad \mathbf{a}_v \cdot \mathbf{a}^u = 0. \quad (36b)$$

The covariant unitary vectors  $\mathbf{a}_u$  and  $\mathbf{a}_v$  are tangential to the  $u$ - and  $v$ -directed edges, respectively. Thus, from (36b) we conclude that the contravariant vectors  $\mathbf{a}^u$  and  $\mathbf{a}^v$  are normal to the  $v$ - and  $u$ -directed edges, respectively. The surface Jacobian is given by  $\mathcal{J}_s = |\mathbf{a}_u \times \mathbf{a}_v|$  and we have the relations

$$\mathbf{a}^u = \frac{1}{\mathcal{J}_s} \mathbf{a}_v \times \hat{\mathbf{n}}, \quad \mathbf{a}^v = \frac{1}{\mathcal{J}_s} \hat{\mathbf{n}} \times \mathbf{a}_u \quad (37)$$

where  $\hat{\mathbf{n}} = \mathbf{a}_u \times \mathbf{a}_v / \mathcal{J}_s$  is the unit normal vector. This also implies that

$$|\mathbf{a}_v| = \mathcal{J}_s |\mathbf{a}^u|, \quad |\mathbf{a}_u| = \mathcal{J}_s |\mathbf{a}^v|. \quad (38)$$

REFERENCES

- [1] R. F. Harrington, *Field Computation by Moment Methods*. New York: Macmillan, 1968.
- [2] *Fast and Efficient Algorithms in Computational Electromagnetics*, W. C. Chew, J. M. Jin, E. Michielssen, and J. Song, Eds., Artech House, Norwood, MA, 2001.

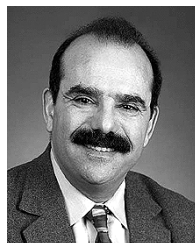
- [3] R. Coifman, V. Rokhlin, and S. Wandzura, "The fast multipole method for the wave equation: A pedestrian prescription," *IEEE Antennas Propagat. Mag.*, vol. 35, no. 3, pp. 7–12, June 1993.
- [4] S. Wandzura, "Electric current basis functions for curved surfaces," *Electromagn.*, vol. 12, pp. 77–91, 1992.
- [5] B. M. Kolundzija and B. D. Popović, "Entire-domain Galerkin method for analysis of metallic antennas and scatterers," *Proc. Inst. Elect. Eng.*, pt. H, vol. 140, no. 1, pp. 1–10, February 1993.
- [6] B. D. Popović and B. M. Kolundzija, *Analysis of Metallic Antennas and Scatterers*. London, U.K.: IEE, 1994.
- [7] K. R. Aberegge, A. Taguchi, and A. F. Peterson, "Application of higher order vector basis functions to surface integral equation formulations," *Radio Sci.*, vol. 31, no. 5, pp. 1207–1213, Sep.–Oct. 1996.
- [8] R. D. Graglia, D. R. Wilton, and A. F. Peterson, "Higher order interpolatory vector bases for computational electromagnetics," *IEEE Trans. Antennas Propagat.*, vol. 45, pp. 329–342, Mar. 1997.
- [9] W. Cai, T. Yu, H. Wang, and Y. Yu, "High-order mixed RWG basis functions for electromagnetic applications," *IEEE Trans. Microwave Theory and Techniques*, vol. 49, pp. 1295–1303, July 2001.
- [10] B. M. Notaroš, B. D. Popović, J. P. Weem, R. A. Brown, and Z. Popović, "Efficient large-domain MoM solution to electrically large EM problems," *IEEE Trans. Microwave Theory and Techniques*, vol. 49, pp. 151–159, Jan. 2001.
- [11] M. Djordjević and B. M. Notaroš, "Three types of higher order MoM basis functions automatically satisfying current continuity conditions," in *Proc. IEEE Antennas Propagat. Soc. Int. Symp.*, vol. IV, San Antonio, TX, June 2002, pp. 610–613.
- [12] J. C. Nedelec, "Mixed finite element in  $R^3$ ," *Numer. Mathem.*, vol. 35, pp. 315–341, 1980.
- [13] A. F. Peterson and D. R. Wilton, *Finite Element Software for Microwave Engineering*, T. Itoh, G. Pelosi, and P. P. Silvester, Eds. New York: Wiley, 1996, ch. 5, pp. 101–124.
- [14] L. S. Andersen and J. L. Volakis, "Development and application of a novel class of hierarchical tangential vector finite elements for electromagnetics," *IEEE Trans. Antennas Propagat.*, vol. 47, pp. 112–120, Jan. 1999.
- [15] J. P. Webb, "Hierarchical vector basis functions of arbitrary order for triangular and tetrahedral finite elements," *IEEE Trans. Antennas Propagat.*, vol. 47, pp. 1244–1253, Aug. 1999.
- [16] S. M. Rao, D. R. Wilton, and A. W. Glisson, "Electromagnetic scattering by surfaces of arbitrary shape," *IEEE Trans. Antennas Propagat.*, vol. AP-30, pp. 409–418, May 1982.
- [17] A. F. Peterson, C. F. Smith, and R. Mittra, "Eigenvalues of the moment-method matrix and their effect on the convergence of the conjugate gradient algorithm," *IEEE Trans. Antennas Propagat.*, vol. 36, pp. 1177–1179, Aug. 1988.
- [18] E. Jørgensen, J. L. Volakis, P. Meincke, and O. Breinbjerg, "Higher order hierarchical Legendre basis functions for iterative integral equation solvers with curvilinear surface modeling," in *Proc. IEEE Antennas Propagat. Soc. Int. Symp.*, vol. IV, San Antonio, TX, June 2002, pp. 618–621.
- [19] M. I. Sancer, R. L. McClary, and K. J. Glover, "Electromagnetic computation using parametric geometry," *Electromagn.*, vol. 10, pp. 85–103, Jan.–June 1990.
- [20] G. E. Antilla and N. G. Alexopoulos, "Scattering from complex three-dimensional geometries by a curvilinear hybrid finite-element-integral equation approach," *J. Opt. Soc. Amer. A*, vol. 11, no. 4, pp. 1445–1457, April 1994.
- [21] J. M. Song and W. C. Chew, "Moment method solutions using parametric geometry," *J. Electromagn. Waves Appl.*, vol. 9, pp. 71–83, 1995.
- [22] R. D. Graglia, "The use of parametric elements in the moment method solution of static and dynamic volume integral equations," *IEEE Trans. Antennas Propagat.*, vol. 36, pp. 636–646, May 1988.
- [23] J. Shen, "Efficient spectral-Galerkin method I. Direct solvers of second- and fourth-order equations using Legendre polynomials," *SIAM J. Sci. Comput.*, vol. 15, no. 6, pp. 1489–1505, Nov. 1994.
- [24] M. G. Duffy, "Quadrature over a pyramid or cube of integrands with a singularity at a vertex," *SIAM J. Numer. Anal.*, vol. 19, no. 6, pp. 1260–1262, Dec. 1982.
- [25] K. Sertel and J. L. Volakis, "Method of moments solution of volume integral equations using parametric geometry," *Radio Sci.*, vol. 37, no. 1, pp. 1–7, Jan.–Feb. 2002.
- [26] B. M. Notaroš and B. D. Popović, "General entire-domain method for analysis of dielectric scatterers," *Proc. Inst. Elect. Eng. Microw. Antennas Propag.*, vol. 143, no. 6, pp. 498–504, Dec. 1996.
- [27] L. R. Hamilton, J. J. Ottusch, M. A. Stalzer, R. S. Turley, J. L. Visher, and S. M. Wandzura, "Accuracy estimation and high order methods," in *Proc. 11th Annual Review of Progress in Applied Computational Electromagnetics*, vol. 2, Mar. 1995, pp. 1177–1184.
- [28] B. M. Kolundzija, "Accurate solution of square scatterer as benchmark for validation of electromagnetic modeling of plate structures," *IEEE Trans. Antennas Propagat.*, vol. 46, pp. 1009–1014, July 1998.
- [29] E. Jørgensen, "Higher order integral equation methods in computational electromagnetics," Ph.D. dissertation, Technical University of Denmark, Ørsted-DTU, Lyngby, Denmark, 2003.
- [30] E. Jørgensen, J. L. Volakis, P. Meincke, and O. Breinbjerg, "Divergence-conforming higher order hierarchical basis functions and preconditioning strategies for boundary integral operators," in *Proc. 6th Int. Workshop on Finite Elements in Microw. Eng.-Book of Abstracts*, Chios, Greece, May 2002, p. 63.
- [31] Y. Saad. (1996) *Iterative Methods for Sparse Linear Systems*. Boston, MA: PWS. [Online]. Available: <http://www-users.cs.umn.edu/~saad/books.html>
- [32] A. F. Peterson, S. C. Ray, and R. Mittra, *Computational Methods for Electromagnetics*. New York: IEEE Press, 1998.



**Erik Jørgensen** (S'98–M'03) was born in 1974 in Denmark. He received the M.S. and Ph.D. degrees in electrical engineering from the Technical University of Denmark, in 2000 and 2003, respectively.

In fall 1998, he spent five months at the University of Siena, Italy. In fall 2001, he was a Visiting Scholar at the Radiation Laboratory, University of Michigan, Ann Arbor. In 2003, he joined the Danish company TICRA, Copenhagen, where he is currently developing software for reflector antenna analysis. His research interests include computational electromag-

netics and high-frequency techniques.



**John L. Volakis** (S'77–M'82–SM'89–F'96) was born on May 13, 1956, in Chios, Greece. He received the B.E. degree (*summa cum laude*) from Youngstown State University, Youngstown, OH, in 1978 and the M.Sc. and Ph.D. degrees from The Ohio State University, Columbus, in 1979 and 1982, respectively.

From 1982 to 1984, he was with Rockwell International, Aircraft Division, Lakewood, CA, and during 1978 to 1982, he was a Graduate Research Associate at the ElectroScience Laboratory, The Ohio State University. Since 1984, has been a Professor in the Electrical Engineering and Computer Science Department, University of Michigan, Ann Arbor, where from 1998 to 2000, he also served as the Director of the Radiation Laboratory. Since January 2003, he has been the Roy and Lois Chope Chair Professor of Engineering at The Ohio State University, Columbus, and also serves as the Director of the ElectroScience Laboratory. He has published over 200 articles in major refereed journal articles (nine of these have appeared in reprint volumes), more than 240 conference papers and nine book chapters. In addition, he coauthored two books *Approximate Boundary Conditions in Electromagnetics* (London, U.K.: IEE, 1995) and *Finite Element Method for Electromagnetics* (New York: IEEE Press, 1998). From 1994 to 1997, he was an Associate Editor of *Radio Science* and is currently an Associate Editor for the *Journal of Electromagnetic Waves and Applications*. His primary research deals with computational methods, electromagnetic compatibility and interference, design of new RF materials, multiphysics engineering and bioelectromagnetics.

Dr. Volakis is a Member of Sigma Xi, Tau Beta Pi, Phi Kappa Phi, and Commission B of the International Scientific Radio Union (URSI). In 1998, he received the University of Michigan College of Engineering Research Excellence award and in 2001 he received the Department of Electrical Engineering and Computer Science Service Excellence Award. He served as an Associate Editor of the IEEE TRANSACTIONS ON ANTENNAS AND PROPAGATION from 1988 to 1992, and is currently an Associate Editor for the IEEE ANTENNAS AND PROPAGATION SOCIETY MAGAZINE and the *URSI Bulletin*. He chaired the 1993 IEEE Antennas and Propagation Society Symposium and Radio Science Meeting, and was a Member of the AdCom for the IEEE Antennas and Propagation Society from 1995 to 1998. He currently serves as the President of the IEEE Antennas and Propagation Society. He is listed in several *Who's Who* directories, including *Who's Who in America*.



**Peter Meincke** (S'93–M'96) was born in Roskilde, Denmark, on November 25, 1969. He received the M.S.E.E. and Ph.D. degrees from the Technical University of Denmark (DTU), Lyngby, Denmark, in 1993 and 1996, respectively.

In spring and summer of 1995, he was a Visiting Research Scientist at the Electromagnetics Directorate of Rome Laboratory, Hanscom Air Force Base, MA. In 1997, he was with a Danish cellular phone company, working on theoretical aspects of radio-wave propagation. In spring and summer of

1998, he was visiting the Center for Electromagnetics Research, Northeastern University, Boston, MA, while holding a Postdoctoral position from DTU. In 1999, he became a staff member of the Department of Electromagnetic Systems, DTU. He is currently an Associate Professor with Ørsted-DTU, Electromagnetic Systems, DTU. His current teaching and research interests include electromagnetic theory, inverse problems, high-frequency and time-domain scattering, antenna theory, and microwave imaging.

Dr. Meincke won the first prize award in the 1996 IEEE Antennas and Propagation Society Student Paper Contest in Baltimore, MD, for his paper on uniform physical theory of diffraction equivalent edge currents and received the 2000 RWP King Paper Award for his paper "*Time-domain version of the physical theory of diffraction*" published in IEEE TRANSACTIONS ON ANTENNAS AND PROPAGATION, February, 1999.



**Olav Breinbjerg** (M'87) was born in Silkeborg, Denmark on July 16, 1961. He received the M.S.E.E. and Ph.D. degrees from the Technical University of Denmark (DTU), Lyngby, Denmark, in 1987 and 1992, respectively.

Since 1991, he has been on the faculty of Ørsted-DTU, Electromagnetic Systems, DTU, where he is now an Associate Professor and Head of the Antenna and Electromagnetics Group comprising also the DTU-ESA Spherical Near-Field Antenna Test Facility. He was a Visiting Research

Scientist at the Rome Laboratory, Hanscom Air Force Base, MA, in fall 1988 and a Fulbright Scholar at the University of Texas, Austin, in spring 1995. His research interests include electromagnetic field theory, asymptotic and computational electromagnetics, antennas, and scattering.